

48 W Continuous-Wave Output From a High-Efficiency Single Emitter Laser Diode at 915 nm

Yuxian Liu¹, Guowen Yang, Yongming Zhao, Song Tang, Yu Lan, Yuliang Zhao², and Abdullah Demir³

Abstract—Improving the power and efficiency of 9xx-nm broad-area laser diodes has a great help in reducing the cost of laser systems and expanding applications. This letter presents an optimized epitaxial structure with high power and conversion efficiency. Laser diodes with 230 μm emitter width and 5 mm cavity length deliver continuous-wave output power up to 48.5 W at 48 A, 30 °C, the highest power reported for 9xx-nm single emitter lasers so far. The slope efficiency is as high as 1.23 W/A due to a low internal optical loss of 0.31 cm^{-1} and a high internal efficiency of 96%. The maximum power conversion efficiency reaches 72.6% at 15.3 W and 67.3% at the operating power of 30 W under a heatsink temperature of 25 °C. Life test results show no failure in 1000 hours for 55 laser diodes.

Index Terms—Semiconductor laser, laser diode, high power, high efficiency, 915 nm.

I. INTRODUCTION

HIGH power 9xx-nm laser diodes (LDs) are widely used as pump sources for fiber lasers and light sources for direct-diode systems in various industrial applications [1], [2], [3], [4]. 915 nm pump LDs are the major choice for fiber lasers because of their broad absorption band for Yb-doped fibers [1], which has a big advantage for working conditions in a large temperature range. A high-performance laser system with an output power of 1-10 kW needs a large quantity (100 to 1000) of pump LDs. The cost of these systems relies dramatically on the LDs, which gives a stringent requirement for the performance, quality, and reliability of the LD chips [5], [6]. LDs with more than 30 W output power combined with power conversion efficiency (PCE) above 65% can provide a cost-effective high-power laser module. The output power is mainly limited by the catastrophic optical

mirror damage (COMD) [7], catastrophic optical bulk damage (COBD) [8], thermal rollover, and other nonlinear phenomena [9], [10], [11]. Various methods have been applied to eliminate these problems in a few decades. Particularly, progress in epitaxial growth technologies, facet cooling [12], [13], [14] and passivation technologies [1], [15] have greatly improved COMD and COBD power levels [5], [16], [17], [18]. Innovative or optimized epitaxial structures have shown advantages for a continuous power increase of GaAs-based LDs [10], [19], [20], [21], [22], [23], [24]. A 9xx-nm high-power LD with 230 μm emitter width was reported to achieve 45 W at 25 °C [25]. Improving the operating power and PCE of the LDs can reduce the cost of the laser systems. Hence, higher slope efficiency and rollover power level, together with a low operating voltage, are critically important to achieve high output power and efficiency.

This letter presents an optimized epitaxial structure with ultralow optical loss (0.31 cm^{-1}) and high slope efficiency for power-efficient LDs. The maximum achievable CW laser power reaches 48.5 W at 48 A, 30 °C. The maximum PCE of 72.6% is achieved at 15.3 W when the operating power is 30 W at 27.5 A with PCE higher than 67% at 25 °C.

II. SIMULATION AND DESIGN

The front facet optical output power P_{out} at room temperature can be expressed as [1], [23]:

$$P_{\text{out}} = \eta_s (I - I_{\text{th}}) \frac{(1 - R_F) \sqrt{\frac{R_B}{R_F}}}{(1 - R_F) \sqrt{\frac{R_B}{R_F}} + (1 - R_B)} \quad (1)$$

$$\eta_s = \eta_i \frac{\alpha_m}{\alpha_i + \alpha_m} \frac{h\nu}{q} \quad (2)$$

where η_s is the slope efficiency, I_{th} is the threshold current, η_i is the internal quantum efficiency, $\alpha_m = -(1/2L) \ln(R_F R_B)$ is the mirror loss (i.e., output coupling) with cavity length L , front facet reflectivity R_F , and back facet reflectivity R_B , α_i is the internal loss, $h\nu$ is the photon energy, and q is the electron charge. Using a combination of numerical simulation and laser design parameters, we analyze the influence of the laser's internal characteristics on its output power. The laser has a 5 mm cavity length, 98% back-facet reflectivity, 2% front-facet reflectivity and an emission wavelength of 915 nm. Figure 1 (a) shows the calculated slope efficiency versus internal optical loss for various internal efficiency values in the range of 90% to 100%. Both low internal optical loss and high internal quantum efficiency significantly improve slope efficiency. To ensure slope efficiency of higher than 1.20 W/A, optical loss of less than $\sim 0.50 \text{ cm}^{-1}$ is required even for internal efficiency of 100%. The circle in this figure shows the experimental result to be discussed in section III.

Manuscript received 5 August 2022; revised 2 September 2022; accepted 10 September 2022. Date of publication 19 September 2022; date of current version 5 October 2022. This work was supported by Dogain Laser Technology (Suzhou) Company Ltd. (Corresponding authors: Guowen Yang; Abdullah Demir.)

Yuxian Liu, Yu Lan, and Yuliang Zhao are with the State Key Laboratory of Transient Optics and Photonics, Xi'an Institute of Optics and Precision Mechanics, Chinese Academy of Sciences, Xi'an 710119, China, and also with the University of Chinese Academy of Sciences, Beijing 100049, China.

Guowen Yang is with the State Key Laboratory of Transient Optics and Photonics, Xi'an Institute of Optics and Precision Mechanics, Chinese Academy of Sciences, Xi'an 710119, China, also with the University of Chinese Academy of Sciences, Beijing 100049, China, and also with Dogain Laser Technology (Suzhou) Company Ltd., Suzhou 215123, China (e-mail: yangguowen@opt.ac.cn).

Yongming Zhao and Song Tang are with Dogain Laser Technology (Suzhou) Company Ltd., Suzhou 215123, China.

Abdullah Demir is with the UNAM-Institute of Materials Science and Nanotechnology, Bilkent University, 06800 Ankara, Turkey (e-mail: abdullah.demir@unam.bilkent.edu.tr).

Color versions of one or more figures in this letter are available at <https://doi.org/10.1109/LPT.2022.3207786>.

Digital Object Identifier 10.1109/LPT.2022.3207786

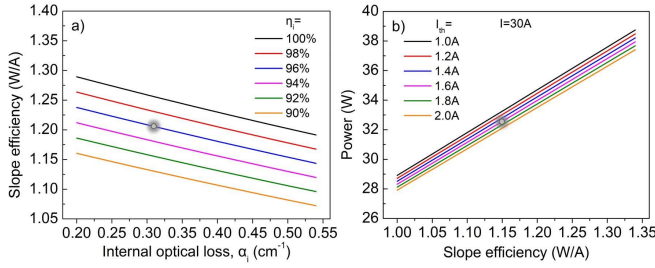


Fig. 1. Calculation results for (a) the slope efficiency versus internal optical loss for various internal efficiency values, and (b) the laser output power at 30 A versus slope efficiency for various threshold current values.

Figure 1(b) shows the calculated output power at 30A as a function of slope efficiency (assuming it is constant) for various threshold current values. It indicates that the slope efficiency substantially impacts the output power compared to the threshold current. Hence, internal optical loss and internal quantum efficiency are critical parameters to achieve high output power at high current levels. Considering the thermal rollover under high current operation with internal efficiency less than 100%, the internal optical loss should be much lower than 0.5 cm⁻¹ based on our calculation results. Therefore, the epitaxial structure design should have a significantly low optical loss to achieve high efficiency for high-power operation.

The internal optical absorption loss can be approximately expressed as the sum of the absorption loss of each layer, j , in the vertical epitaxial structure:

$$\alpha_i = \sum_j \Gamma_j (\sigma_n n_j + \sigma_p p_j) \quad (3)$$

where Γ_j is the optical confinement factor; n_j and p_j are the electron and hole carrier concentrations, respectively. σ_n and σ_p are the free carrier absorption coefficients for electrons and holes, respectively. The absorption coefficients are assumed to be equal to the GaAs bulk material as $\sigma_n = 4 \times 10^{-18}$ cm² and $\sigma_p = 12 \times 10^{-18}$ cm², respectively [21].

GaAs-based epitaxial structure is optimized by considering the following key factors:

- 1) A novel asymmetric structure with thin p-waveguide and thick n-waveguide layers is designed to locate most of the optical mode on the n-side and minimize the optical loss due to the low free carrier absorption loss of the electrons. In the meantime, thin p-waveguide and p-cladding layers reduce the series resistance, leading to low thermal resistance and bias-driven leakage currents.
- 2) The doping level is optimized to minimize the overlap of high doping and high mode intensity for lower internal optical absorption loss but balanced to avoid high series resistance.
- 3) A modest optical confinement factor of QW is employed to suppress COMD at a high power with high Γ_{QW} and avoid high optical loss caused by high carrier density in the quantum well with low Γ_{QW} .
- 4) The AlGaAs compositions are adjusted to avoid high-order mode lasing in the vertical direction.
- 5) A compressively-strained QW lasing at 915 nm is used to achieve high gain. A suitable QW barrier is introduced to improve the internal quantum efficiency and temperature stability by reducing the carrier leakage from the QW. The compositions of the QW and barrier materials

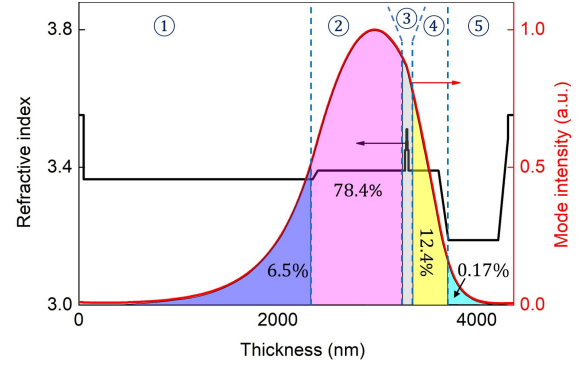


Fig. 2. Simulation result for the refractive index profile of the epitaxial structure and the vertical near-field profile.

for high-quality growth are also considered to achieve high internal quantum efficiency and low internal optical absorption loss.

Figure 2 illustrates the calculated refractive index profile and the fundamental mode's intensity. The vertical near-field profile of the fundamental mode is divided into five parts. The optical confinement factors (i.e., Γ) are correspondingly (1) 6.5% for n-cladding, (2) 78.4% for n-waveguide, (3) 2.6% for the region with QW ($\Gamma_{QW} = 0.63\%$) and QW-barrier, (4) 12.4% for the p-waveguide, and 0.17% for the p-cladding. The optical confinement factor ratio of p-region to n-region is as low as 14.8%, resulting in an extremely low optical absorption loss of 0.32 cm⁻¹ based on the simulation.

The epitaxial structure is grown by MOCVD on a GaAs substrate. To make a laser diode, the ridge is firstly formed by wet etching. Then an insulating layer is deposited by plasma-enhanced chemical vapor deposition (PECVD), followed by a window opening for current injection. P-metal and n-metal depositions are carried out on the top and bottom surfaces of the wafer, respectively. The wafer is finally cleaved into bars and a facet-passivation technique is employed to improve the COMD level. Lasers with various cavity lengths are left uncoated to determine the internal parameters of the laser diode. For performance measurements, the front and back facets are coated with anti-reflective and high-reflective films, respectively. Finally, the bars are cleaved into single devices, mounted in a p-side down configuration with hard solder on high thermal conductivity AlN submounts bonded on top of Cu heatsinks. Single emitters are designed with a 5 mm cavity length and 230 μ m waveguide width targeting high output operation power.

III. RESULTS

Firstly, uncoated devices with 200 μ m stripe width and four different cavity lengths from 2 mm to 3.5 mm were measured under pulsed operation with a low duty cycle (pulse width of 100 μ s, repetition rate of 100 Hz) to extract the internal parameters of the epitaxial structure. The dependencies of the inverse differential quantum efficiency ($1/\eta_d$) on the cavity length (L) and the logarithm of the threshold current density ($\ln(J_{th})$) on the inverse cavity length ($1/L$) are shown in Fig. 3(a) and 3(b), where each data point represents one chip.

Assuming uncoated facet reflectivity as $R_F = R_B = 0.3$ and using linear fitting of the results [23], the internal efficiency η_i , internal optical losses α_i , transparency current density J_{tr} , and modal gain coefficient ΓG_0 are extracted to be 96%, 0.31 cm⁻¹, 77.36 A/cm², and 8.67 cm⁻¹, respectively.

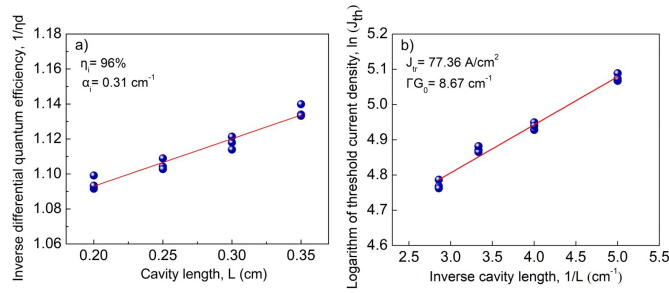


Fig. 3. Experimental results under pulsed operation for (a) the inverse differential quantum efficiency versus cavity length and (b) the natural logarithm of threshold current density versus inverse cavity length.

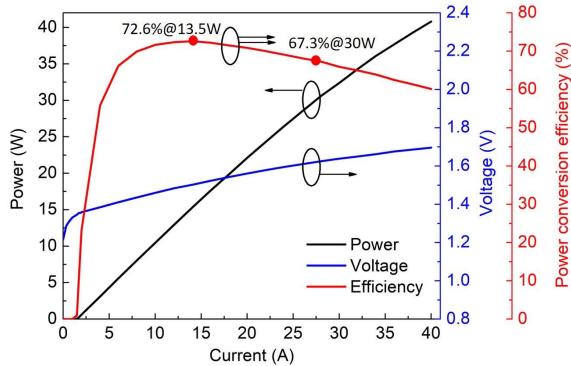


Fig. 4. Power, voltage and efficiency versus current curves at 25 °C under CW operation.

The calculated experimental value of the 0.31 cm^{-1} for the internal optical loss agrees well with the simulation result of 0.32 cm^{-1} . The low transparency current density shows high material quality, and a relatively low modal gain with the calculated confinement factor of 0.63% gives a G_0 value of 1376 cm^{-1} .

Figure 4 demonstrates the power, voltage, and PCE curves of a typical single emitter under the CW operation at 25 °C. The laser output powers were measured with a calibrated thermopile sensor (F150-BB-26) and Ophir NOVA II power meter. A recorded high power of 40.8 W is achieved at 40 A (Higher current is limited by the temperature control capability of the TEC at 25 °C) without sudden catastrophic failure and thermal rollover of the output power. The maximum PCE is as high as 72.6% at 14 A with an output power of 15.3 W. The slope efficiency and threshold of the devices are 1.23 W/A and 1.5 A obtained by linear fitting of LI curve between 2 and 10 A, respectively. The series resistance is 9.4 mΩ by linear fitting of the VI curve between 6 and 30 A. 32.4 W output was achieved at 30 A with a high slope efficiency of 1.15 W/A between 1.6 and 30 A, which coincided nicely with the calculated value of 32.7 W presented in Fig. 1(b). A high PCE of more than 67% is achieved up to 30 W at 27.5 A.

Figure 5(a) shows the vertical and lateral far-field profiles at the operating power of 30 W. The vertical far-field divergence angle with 95% power intensity is nearly 46° . The lateral far-field angle with 95% power intensity is as low as 8.1° at 30 W. Figure 5(b) illustrates the measured lateral divergence angle as a function of current at 25 °C. The lateral divergence angle increases almost linearly from 4 to 30 A, most likely due to the low thermal lensing and high PCE. The lateral far-field angle is less than 9° even at 30 A, which shows high brightness and

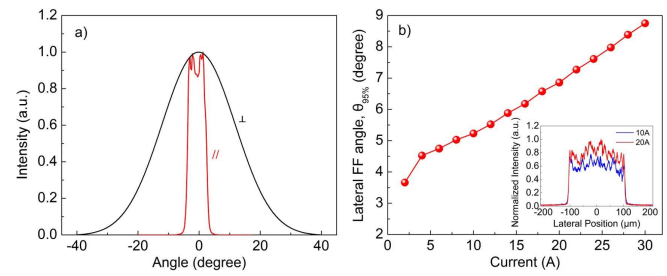


Fig. 5. Experimental results at 25 °C: (a) vertical and lateral divergence angle at 30 W, (b) lateral FF angle versus current. The inset is the near-field at 10 and 20 A, 25 °C.

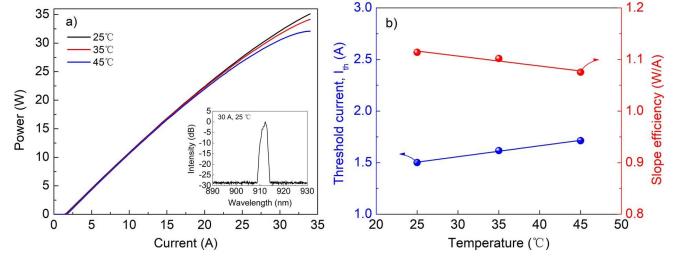


Fig. 6. Testing data under CW operation: (a) L-I curves at 25, 35, and 45 °C (the inset shows the optical spectrum at 30 A, 25 °C), (b) threshold current and slope efficiency versus heatsink temperature (dots represent the measurement data and lines are the fitting curves).

is beneficial to achieving high coupling efficiency. Figure 5(b) inset shows the near-field profile at 10 and 20 A under 25 °C (test current is limited by the current source). The near-field profiles are relatively uniform, and the near-field width with 95% intensity ($W_{95\%}$) is approximately $225 \mu\text{m}$ at 10 and 20 A.

Figure 6(a) shows the L-I curves up to 34 A before apparent power rollover under CW operation at 25, 35, and 45 °C. The inset shows a typical optical spectrum at 30 A with a lasing wavelength of around 915 nm. The maximum output at 35 and 45 °C still maintains high power levels, which are more than 34 and 32 W, respectively. Temperature-dependent parameters T_0 and T_1 can be obtained by:

$$\eta_s(T) = \eta_s(T_{hs}) \exp\left(-\frac{T - T_{hs}}{T_1}\right) \quad (4)$$

$$I_{th}(T) = I_{th}(T_{hs}) \exp\left(\frac{T - T_{hs}}{T_0}\right) \quad (5)$$

where T_{hs} is the heatsink temperature. T_0 and T_1 are the characteristic temperatures for the threshold current and slope efficiency, respectively. Figure 6(b) shows the change of threshold current and slope efficiency as a function of heatsink temperature using linear fitting from 2 to 10 A and 10 to 25 A, respectively. The T_0 and T_1 characteristic temperatures are 152 K and 567 K for the heatsink temperature range of 25–45 °C.

We have explored the power limitation for the laser diodes further, although the TEC is limited to control the temperature at 25 °C beyond 40 A operation current because of the significant heat dissipation. Figure 7(a) presents the CW L-I curves of 10 single emitter lasers up to 53 A, demonstrating relatively similar output power levels. Although the heatsink temperature was set as 20 °C, it increased with the current and reached around 30 °C at the maximum current. All the LDs show power rollover around 49 A without catastrophic optical damage (COD) and reach the rollover output power

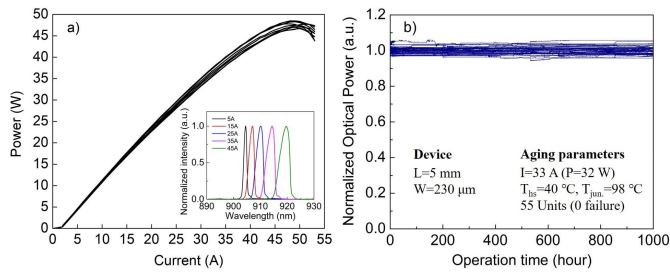


Fig. 7. (a) Power of 10 single emitter lasers versus current under CW test to rollover (the inset shows the spectra at 5/15/25/35/45 A); (b) Accelerated lifetime test 55 laser diodes at 33 A and 40 °C with 32 W output power.

of more than 47 W. The maximum power is 48.5 W at 48 A (at 30 °C), which is expected to be higher if the heatsink could be well controlled at 25 °C. Figure 7(a) inset shows the spectral characteristics of the LD from 5 to 45 A with 10 A steps. The calculated current drift coefficient is about 0.36 nm/A. The full width at half-maximum (FWHM) of the spectra is broadened from 1.3 nm at 5 A to 4.2 nm at 45 A, possibly due to the thermal effects and carrier non-pinning [11]. The spectra are compatible with the broad absorption band of Yb-doped fibers in 915±10 nm.

Life tests were also implemented to investigate the long-term operation condition since reliability is crucial to evaluate the success of epitaxial design and fabrication process. Fifty-five chip-on-submount devices were used for the accelerated lifetime test under a constant injection current of 33 A at a heatsink temperature of 40 °C. The output power is 32 W, and the junction temperature is estimated as 98 °C. As shown in Fig. 7(b), 1000 hours of accelerated life testing have been completed without failure. The output power of all the devices has less than 3% variation during the reliability test, which confirms the high reliability of these devices at high currents.

IV. CONCLUSION

We have presented a high output power and high conversion efficiency laser diode operating at 915 nm by investigating the influence of the laser's internal parameters on its output. The asymmetric epitaxial structure is optimized to achieve low optical loss while considering high internal efficiency, low series resistance, and modest optical confinement factor. Experimental results show an internal optical loss of 0.31 cm⁻¹ and internal efficiency of 96%. Laser diodes with 230 μm emitter width and 5 mm cavity length have T₀ and T₁ characteristic temperatures of 152 and 567 K, respectively. Under CW operation, the maximum power conversion efficiency is 72.6% at 15.3 W, and the maximum output is 48.5 W at 48 A (at 30 °C), the highest power reported for a 9xx-nm single emitter laser. At the operating power of 30 W at 25 °C, the power conversion efficiency is 67.3%, and the lateral far-field angle with 95% power content is around 8°.

ACKNOWLEDGMENT

The authors would like to thank all technical experts and employees of Dogain Laser Technology involved in device fabrication.

REFERENCES

[1] P.-W. Epperlein, *Semiconductor Laser Engineering, Reliability and Diagnostics: A Practical Approach to High Power and Single Mode Devices*. West Sussex, U.K.: Wiley, 2013.

[2] E. Zucker *et al.*, "Advancements in laser diode chip and packaging technologies for application in kW-class fiber laser pumping," *Proc. SPIE*, vol. 8965, Mar. 2014, Art. no. 896507.

[3] V. Rossin *et al.*, "High power, high brightness diode lasers for kW lasers systems," in *Proc. IEEE High Power Diode Lasers Syst. Conf. (HPD)*, Oct. 2015, pp. 35–36.

[4] Y. Kasai, T. Aizawa, and D. Tanaka, "High-power fiber-coupled pump lasers for fiber lasers," *Proc. SPIE*, vol. 10514, Feb. 2018, Art. no. 105140J.

[5] H. Naito *et al.*, "Long-term reliability of 915-nm broad-area laser diodes under 20-W CW operation," *IEEE Photon. Technol. Lett.*, vol. 27, no. 15, pp. 1660–1662, Aug. 1, 2015.

[6] K. Yoshikazu, K. Yoshida, Y. Yamagata, R. Nogawa, Y. Yamada, and M. Yamaguchi, "Enhanced power conversion efficiency in 900-nm range single emitter broad stripe laser diodes maintaining high power operability," *Proc. SPIE*, vol. 10900, Mar. 2019, Art. no. 109000F.

[7] J. W. Tomm, M. Ziegler, M. Hempel, and T. Elsaesser, "Mechanisms and fast kinetics of the catastrophic optical damage (COD) in GaAs-based diode lasers," *Laser Photon. Rev.*, vol. 5, no. 3, pp. 422–441, Mar. 2011.

[8] Y. Sin, Z. Lingley, N. Presser, M. Brodie, N. Ives, and S. C. Moss, "Catastrophic optical bulk damage in high-power InGaAs-AlGaAs strained quantum well lasers," *IEEE J. Sel. Topics Quantum Electron.*, vol. 23, no. 6, pp. 1–13, Nov. 2017.

[9] J. Piprek and Z. Li, "What causes the pulse power saturation of GaAs-based broad-area lasers?" *IEEE Photon. Technol. Lett.*, vol. 30, no. 10, pp. 963–966, May 15, 2018.

[10] A. Demir, M. Peters, R. Duesterberg, V. Rossin, and E. Zucker, "Semiconductor laser power enhancement by control of gain and power profiles," *IEEE Photon. Technol. Lett.*, vol. 27, no. 20, pp. 2178–2181, Oct. 15, 2015.

[11] T. Kaul, G. Erbert, A. Klehr, A. Maasdorf, D. Martin, and P. Crump, "Impact of carrier nonpinning effect on thermal power saturation in GaAs-based high power diode lasers," *IEEE J. Sel. Topics Quantum Electron.*, vol. 25, no. 6, pp. 1–10, Nov. 2019.

[12] S. Arslan, S. Gundogdu, A. Demir, and A. Aydinli, "Facet cooling in high-power InGaAs/AlGaAs lasers," *IEEE Photon. Technol. Lett.*, vol. 31, no. 1, pp. 94–97, Jan. 1, 2019.

[13] K. Ebadi *et al.*, "Multisection waveguide method for facet temperature reduction and improved reliability of high-power laser diodes," *Proc. SPIE*, vol. 12141, May 2022, Art. no. 1214104.

[14] Y. Liu *et al.*, "Elimination of catastrophic optical mirror damage in continuous-wave high-power laser diodes using multi-section waveguides," *Opt. Exp.*, vol. 30, no. 18, pp. 31539–31549, Aug. 2022.

[15] Y. Lan, G. Yang, Y. Zhao, Y. Liu, and A. Demir, "Facet passivation process of high-power laser diodes by plasma cleaning and ZnO film," *Appl. Surf. Sci.*, vol. 596, Sep. 2022, Art. no. 153506.

[16] L. J. Mawst, H. Kim, G. Smith, W. Sun, and N. Tansu, "Strained-layer quantum well materials grown by MOCVD for diode laser application," *Prog. Quantum Electron.*, vol. 75, Jan. 2021, Art. no. 100303.

[17] P. Ressel *et al.*, "Novel passivation process for the mirror facets of Al-free active-region high-power semiconductor diode lasers," *IEEE Photon. Technol. Lett.*, vol. 17, no. 5, pp. 962–964, May 2005.

[18] R. W. Lambert *et al.*, "Facet-passivation processes for the improvement of Al-containing semiconductor laser diodes," *J. Lightw. Technol.*, vol. 24, no. 2, pp. 956–961, Feb. 2006.

[19] P. Crump *et al.*, "Efficient high-power laser diodes," *IEEE J. Sel. Topics Quantum Electron.*, vol. 19, no. 4, Feb. 2013, Art. no. 1501211.

[20] Z. Wang, T. Li, G. Yang, and Y. Song, "High power, high efficiency continuous-wave 808 nm laser diode arrays," *Opt. Laser Technol.*, vol. 97, pp. 297–301, Dec. 2017.

[21] T. Kaul, G. Erbert, A. Maaßdorf, S. Knigge, and P. Crump, "Suppressed power saturation due to optimized optical confinement in 9xx nm high-power diode lasers that use extreme double asymmetric vertical designs," *Semicond. Sci. Technol.*, vol. 33, no. 3, Jan. 2018, Art. no. 035005.

[22] Y. Yamagata, Y. Kaifuchi, R. Nogawa, K. Yoshida, R. Morohashi, and M. Yamaguchi, "Highly efficient 9xx-nm band single emitter laser diodes optimized for high output power operation," *Proc. SPIE*, vol. 11262, Mar. 2020, Art. no. 1126203.

[23] Y. Liu *et al.*, "High-power operation and lateral divergence angle reduction of broad-area laser diodes at 976 nm," *Opt. Laser Technol.*, vol. 141, Sep. 2021, Art. no. 107145.

[24] Y. Lan *et al.*, "808 nm broad-area laser diodes designed for high efficiency at high-temperature operation," *Semicond. Sci. Technol.*, vol. 36, no. 10, Sep. 2021, Art. no. 105012.

[25] J. Wang *et al.*, "Volume manufacturing of high-power diode lasers using 6" wafers," *Proc. SPIE*, vol. 11983, Mar. 2022, Art. no. 1198306.